# **Fast Channel Simulation via Error-Correcting Codes**

Sharang M. Sriramu School of ECE Cornell University Ithaca, NY 14853

sms579@cornell.edu

Rochelle Barsz School of ECE Cornell University Ithaca, NY 14853 rsb359@cornell.edu Elizabeth Polito School of ECE Cornell University Ithaca, NY 14853 emp234@cornell.edu

Aaron B. Wagner School of ECE Cornell University Ithaca, NY 14853 wagner@cornell.edu

## **Abstract**

We consider the design of practically-implementable schemes for the task of channel simulation. Existing methods do not scale with the number of simultaneous uses of the channel and are therefore unable to harness the amortization gains associated with simulating many uses of the channel at once. We show how techniques from the theory of error-correcting codes can be applied to achieve scalability and hence improved performance. As an exemplar, we focus on how polar codes can be used to efficiently simulate i.i.d. copies of a class of binary-output channels.

## 1 Introduction

Channel simulation refers to the task in which Alice observes a realization x of a random variable X and sends a bit string to Bob. Bob, who shares common randomness with Alice, outputs a random variable Y using both the message and the common randomness. The goal is to minimize the length of the bit string subject to the constraint that Y should have a specified distribution  $P_{Y|X}(\cdot|x)$ . This problem can be viewed as a "soft" or "stochastic" generalization of quantization. As with quantization, Y has a digital representation (through Alice's message), and it can be viewed as a degraded version of X. The difference is that here the degrading process is stochastic in general. In fact, the quantization problem is subsumed by taking the channel  $P_{Y|X}$  to be deterministic.

This stochastic generalization of quantization arises in lossy compression of various types of sources including images [Flamich et al., 2020, Ballé et al., 2020], models [Havasi et al., 2018], and gradients [Shah et al., 2022]. In these applications, X often represents a vector of latent variables, model weights, or even an image consisting of millions of pixels [Theis et al., 2022]. The channel of interest is therefore high dimensional, and it is usually independent across the dimensions. For conventional quantization, it has long been recognized that the optimum rate-distortion tradeoff is more favorable in higher dimensions [Cover and Thomas, 2006], a trend that one expects to generalize to channel simulation. Indeed, let  $n \cdot R_n$  be the minimum number of bits required to generate  $Y^n = (Y_1, \ldots, Y_n)$ , when  $X^n$  is i.i.d. and  $Y^n$  is conditionally i.i.d. given  $X^n$ . Thus  $R_n$  is the minimum number of bits per dimension when simulating the channel n times. The sequence  $nR_n$ 

107932

38th Conference on Neural Information Processing Systems (NeurIPS 2024).

can be shown to be *subadditive* and therefore satisfies (e.g., Liggett [1999, Thm. B22])

$$\lim_{n \to \infty} R_n = \inf_n R_n. \tag{1}$$

It is known that  $R_1$  satisfies [Li and El Gamal, 2018]

$$I(X;Y) \le R_1 \le I(X;Y) + \log(I(X;Y) + 1) + 5,$$
 (2)

where I(X;Y) refers to conventional Shannon mutual information. Applying this to i.i.d.  $(X^n,Y^n)$  and using the fact that  $I(X^n;Y^n)=nI(X;Y)$ , we have

$$nI(X;Y) \le n \cdot R_n \le nI(X;Y) + \log(nI(X;Y) + 1) + 5,$$
 (3)

which shows that as  $n \to \infty$ ,  $R_n$  approaches the lower bound I(X;Y). The challenge, for both quantization and channel simulation, is that the complexity of schemes tends to grow exponentially in n. In fact, although many channel simulation schemes have been proposed [Harsha et al., 2007], [Li and El Gamal, 2018], [Flamich et al., 2022], [Flamich and Theis, 2023], [Flamich et al., 2024], none have complexity that scales subexponentially in n, ignoring isolated examples for which  $R_1$  happens to equal I(X;Y) [Zamir and Feder, 1992], [Agustsson and Theis, 2020].

Vector quantization has long been recognized to be the dual, in a precise sense, of channel coding [Pradhan et al., 2003]. In channel coding, the decoder maps an arbitrary point to an element of a finite set that is "close" in some channel-dependent sense. This is analogous to the role of the encoder in quantization. Likewise, the encoder in channel coding is analogous to the decoder in quantization: both map bit strings to elements of said discrete set. Thus new techniques for channel coding can often be applied to vector quantization [Goblick, 1963], [Viterbi and Omura, 1974] and vice versa [Laroia et al., 1994].

The goal of this paper is to demonstrate how ideas from coding theory can be applied to the channel simulation problem. We shall see that by adopting these techniques, we can develop schemes that significantly outperform state-of-the art methods, both in terms of their scalability and their rate performance. Specifically, we show how polar codes [Arikan, 2009] can be applied to the simulation problem using a method called PolarSim. Polar codes make for a good exemplar of this general proposal for five reasons. First, they have excellent channel coding performance, both theoretically [Mondelli et al., 2016] and practically [Egilmez et al., 2019]. Second, their complexity scales as  $n \log n$ . Third, they require no manual tuning. Fourth, they are simple to describe, requiring minimal background in coding theory. Finally, there exist highly optimized implementations of the encoding and decoding algorithms (e.g., [Pfister, 2023]). Their limitation is that, in their basic form, they can only be applied to symmetric binary-input channels (see (4) to follow). As we shall see, this means that PolarSim can only simulate symmetric binary-output channels. This class includes, for example, the binary symmetric channel, the (reverse) binary erasure channel, and channels of the form  $X \to \operatorname{signum}(X+Z)$ , where X and Z are real-valued, independent random variables with symmetric distributions. Note that the input to the channel need not be binary and may even be continuous.

For these channels, we show both theoretically and experimentally that, by scaling up the dimension, the rate of PolarSim can be made to approach the mutual information lower bound  $I(X;Y) \leq R_n$  from (3). The superior scalability of PolarSim thus translates to a significant rate improvement over the state-of-the-art, since those schemes are not able to harness the amortization gain associated with letting n grow. Although PolarSim is restricted to binary-output channels, it is worth noting that there are currently no known schemes that simulate any nontrivial class of channels with even subexponential complexity in n. Also, for compression applications, a binary output alphabet is not unreasonable. It should be emphasized that the binary-output restriction is particular to the basic form of polar codes, not error-correction methods in general. In the supplementary materials we discuss how a different coding technique, trellis coded modulation, can be applied to closely simulate a Gaussian channel. See also the discussion in the Concluding Remarks section on non-binary polar codes.

One lesson from the coding theory literature, especially with the advent of modern coding theory in the 1990s [Richardson and Urbanke, 2008], is that it is advantageous to prioritize scalability with the dimension n over achieving optimal performance for particular n. The reason is that performance naturally improves with increasing n (as in (1)-(3) above), and this improvement can overcome suboptimality at any given value of n. For state-of-the-art channel codes, the decoder typically does not implement the optimal (maximum likelihood) decision rule. Instead, it implements a

scalable approximation to it. This design strategy of favoring scalability over optimality is now well established in coding theory and vector quantization, and our goal here is to show how it can be profitably applied to channel simulation.

The rest of the paper is organized as follows. We provide the necessary background on polar codes in Section 2. Section 3 describes the PolarSim scheme, with Section 3.3 containing the theoretical result and Section 3.4 contains simulation results. Some concluding remarks are offered in Section 5.

### 1.1 Terminology and Notation

We follow the standard convention of denoting the dimensionality of vectors by their superscript. We will also denote compound i.i.d. channels by superscripts:  $p^{\times n}$  denotes n i.i.d. copies of a distribution p. The number of copies here is referred to as the *block length* or *dimension* of the channel. This is to be distinguished from the notation  $F^{\otimes n}$  which denotes a n-fold self-Kronecker product of a tensor F. All logarithms mentioned in this paper are base 2. The *binary entropy function*  $h_B: [0, \frac{1}{2}] \mapsto [0, 1]$  is defined as  $h_B(p) = -p \log p - (1-p) \log (1-p)$ . We will also refer to its inverse  $h_B^{-1}: [0, 1] \mapsto [0, \frac{1}{2}]$  defined such that  $h_B^{-1}(h_B(p)) = p$ .

# 2 Background

#### 2.1 The Channel Simulation Problem

Consider a joint probability measure  $p_{XY}$  on the set  $\mathcal{X} \times \mathcal{Y}$ . Alice receives a sequence of n symbols from the input alphabet  $\mathcal{X}$  drawn according to  $p_X^{\times n}$  and encodes it into a binary string that she transmits to Bob. Upon receiving the message from Alice, Bob then decodes it to generate a sample from the channel  $p_{Y|X}^{\times n}$ . The objective is to find coding schemes that minimize the average rate—i.e., the average amortized length of the bit string transmitted by Alice. We refer to n as the block length or the dimension. We require that the set of strings that Alice can transmit to Bob to form a prefix-free set, meaning that no string in the set is a prefix of any other. Alice's message is thus self-terminating, and schemes for block length m and n can be combined to obtain a scheme for block length m+n by concatenation. If  $R_n$  denotes the minimum average rate, i.e., the minimum average length of Alice's string over all schemes, normalized by n, then  $nR_n$  is subadditive in n, as noted earlier.

Both Alice and Bob are permitted to use randomized strategies and are assumed to share a source of common randomness. Under this assumption, Li and El Gamal [2018] prove the performance bounds (2) and (3) above (see also Harsha et al. [2007]). For large n, Sriramu and Wagner [2024] improve upon this result for i.i.d. discrete memoryless channels, showing that the logarithmic redundancy term can be halved for some channels and eliminated for all others. While these schemes are nearly rate-optimal, their complexity scales exponentially in n. Other practical schemes have been proposed, although none have even subexponential scaling in n outside the small class of channels for which the lower bound in (3) is tight for all n.

# 2.2 Background on Polar Codes

Modern coding theory has focused on the search for codes whose rates approach the theoretical limit while having a low encoding and decoding complexity. *Polar codes* are among the crowning achievements of this search. In their basic form, they are capacity-achieving linear codes for binary input channels  $W_{X|Y}(\cdot|\cdot)$  satisfying the following symmetry condition: there exists a bijection  $\pi:\mathcal{X}\mapsto\mathcal{X}$  such that  $\pi^{-1}=\pi$  and

$$W(x|0) = W(\pi(x)|1) \text{ for all } x \in \mathcal{X}.$$
(4)

As a linear code, the encoding procedure for polar codes is defined by a generator matrix  $G_n$  that maps an input  $U^n \in \{0,1\}^n$  to the channel input  $Y^n$  as  $Y^n = U^n G_n$  with all operations performed over  $\mathbb{F}_2$ . The generator matrix of size  $n=2^m$  can be constructed recursively from a kernel matrix  $F=\begin{bmatrix}1&0\\1&1\end{bmatrix}$  and the "bit-reversal" permutation matrix  $B_n$ —see Arikan [2009]. The generator matrix is then defined as  $G_n=B_nF^{\otimes n}$ . The structure of the generator matrix allows for encoding in  $n\log n$  time.

Decoding proceeds by sequentially guessing each bit of  $U^n$  in order. For this, one considers the subchannel  $U_i \to (U^{i-1}, X^n)$ . Specifically, given the realization of the output  $x^n$  and the decoding

decisions for the prior bits  $\hat{u}^{i-1}$ , one computes the likelihood ratio

$$\frac{\Pr(U_i = 1 | X^n = x^n, U^{i-1} = \hat{u}^{i-1})}{\Pr(U_i = 0 | X^n = x^n, U^{i-1} = \hat{u}^{i-1})},$$
(5)

and selects  $\hat{U}_i$  accordingly. This decoding rule is suboptimal but scalable in that the likelihood ratio can be computed in  $\log n$  steps using the recursive structure of  $G_n$  [Arikan, 2009], resulting in decoding complexity of  $n \log n$ .

The suboptimality turns out to be acceptable because as n grows, the subchannels polarize, meaning that for most i the likelihood ratio in (5) is close to 0, 1 or  $\infty$  with high probability. Equivalently, the mutual information  $I(U_i; X^n, U^{i-1})$  is close to zero or one. Figure 1 illustrates this phenomenon for a  $binary \ symmetric \ channel$  (BSC) which is defined by  $X = Y \oplus Z$ , where  $Z \sim Bernoulli(p)$  for some crossover probability  $p \in [0,1]$ .

For communication, the encoder uses the "clean" subchannels with mutual information close to 1 to send information bits. The inputs to the remaining noisy channels, called the *frozen bits*, are fixed ahead of time and known to both the encoder and decoder. The data rate is thus the fraction of subchannels that are clean, which can be shown to approach capacity [Arikan, 2009].

Implementing the code requires determining which indices correspond to the clean subchannels. This can be done using the dimensionality reduction technique of Tal and Vardy [2013], by exploiting the recursive structure of the polar transform [Zhang et al., 2014, Arikan, 2009], or by Monte Carlo simulation.

# 3 Simulating Binary Output Channels

Previously, we described polar codes for constructing channel codes for binary *input* channels. Based on the duality between channel coding and channel simulation, we will see that this naturally leads to a scheme for simulating binary *output* channels.

We begin by describing a "toy scheme". This is not a rate-efficient scheme in its own right, but it serves as a foundation for PolarSim.

# 3.1 Toy Scheme for Binary Output Channel Simulation

Consider a joint distribution  $p_{XY}$  where  $p_Y$  is Bernoulli  $(\frac{1}{2})$ . Then, the following algorithm simulates  $p_{Y|X}$  exactly:

- 1. Use the common randomness to generate  $Z \sim \mathrm{Unif}(0,1)$  and  $V = \mathbf{1}\left(Z > \frac{1}{2}\right)$  at both the encoder and decoder.
- 2. At the encoder, having observed an input realization x, compute the output bit  $Y = \mathbf{1}(Z > p_{Y|X}(0|x))$  and the correction bit  $\Delta = Y \oplus V$ .
- 3. Transmit  $\Delta$  to the decoder after lossless compression.
- 4. Recover  $Y = \Delta \oplus V$  at the decoder.

In Appendix A, we show that the rate associated with repeated application of this scheme is upper bounded by  $h_B\left(\frac{1}{2}-h_B^{-1}(1-I(X;Y))\right)$ . As we can see in Figure 2, this is highly suboptimal in general. However, we note that for the special case in which the mutual information is *polarized*, i.e., where  $I(X;Y)\approx 0$  or  $I(X;Y)\approx 1$ , the toy scheme is close to optimal.

This observation is crucial as it suggests a path forward: If we can transform a given channel simulation problem to the problem of simulating polarized channels, it can be solved rate-efficiently using the toy scheme. Polar codes provide us with the means to achieve such a transformation.

# 3.2 Channel Simulation using Polar Codes

As in the toy scheme, we shall consider a joint distribution  $p_{XY}$  where  $p_Y$  is Bernoulli  $\left(\frac{1}{2}\right)$ . We will additionally assume that  $p_{X|Y}$  satisfies the symmetry condition described in (4). Let us then examine

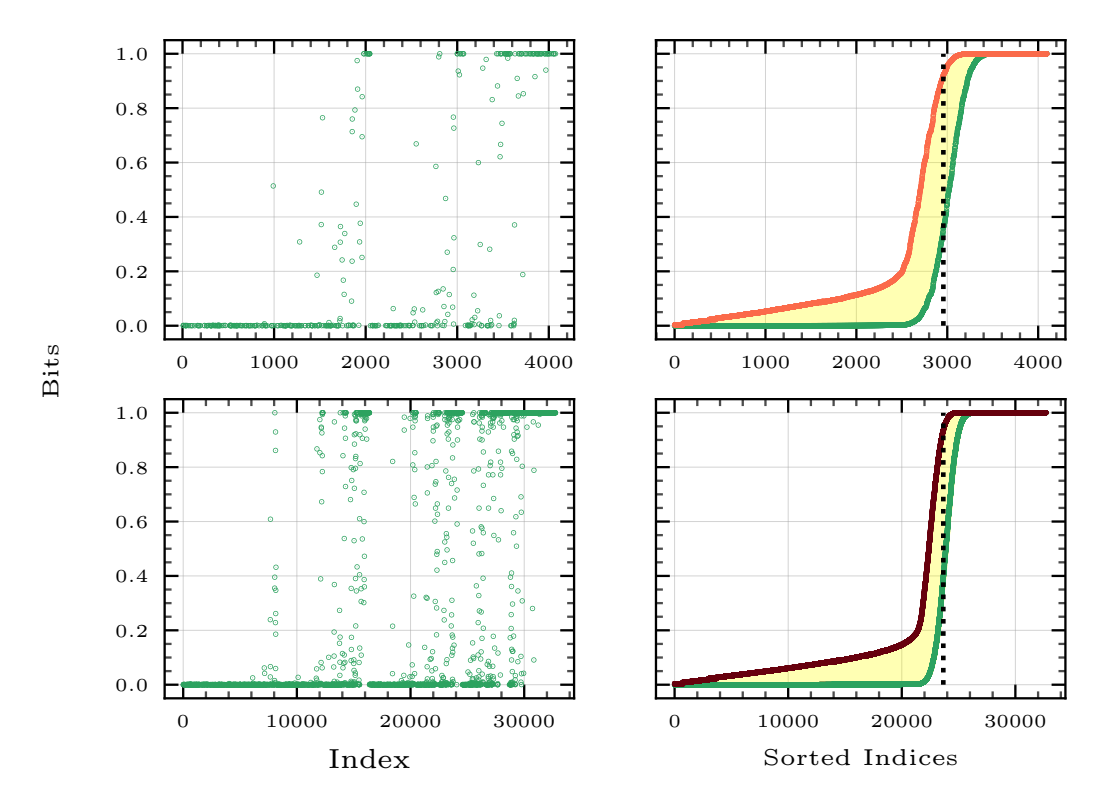
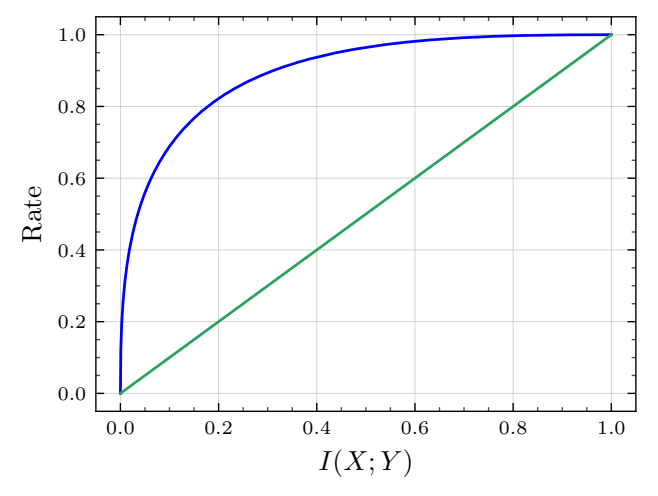


Figure 1: Channel polarization for a BSC with crossover probability 0.2 and block lengths  $n=2^{12}$  (top) and  $n=2^{15}$  (bottom). The scatter plots on the left show the subchannel capacities  $I(U_i;X^n,U^{i-1})$  for each index i. In the curves ( ) on the right, these indices are sorted in the increasing order of their subchannel capacities for better visualization. The area under these curves is the mutual information lower bounds at their respective block length. The vertical dotted line marks the ideal polarized channel, i.e., the fraction of indices to its right is equal to the mutual information of the channel. We see that the sorted subchannel capacity curve approaches this line as the block length is increased. Finally, we also plot the theoretical upper bound (see (38)) on the rate of our proposed scheme, PolarSim, for block lengths  $n=2^{12}$  and  $n=2^{15}$ . The area under these curves is an upper bound on the rate of PolarSim. The shaded area in between is therefore an upper bound on the redundancy of PolarSim, which vanishes as  $n\to\infty$  due to the polarization phenomenon.



**Figure 2:** The upper bound on the rate of the toy scheme (■) described in section 3.1 is plotted against the mutual information lower bound (■).

the problem of simulating two independent realizations of the channel  $p_{Y|X}$ ,  $X^2 \to Y^2$ . Consider the following bijection applied to the output  $(Y_1, Y_2)$ :

$$U_1 = Y_1 \oplus Y_2,$$

$$U_2 = Y_2.$$
 (6)

It is clear that simulating the original pair of i.i.d. channels  $X_1 \to Y_1$  and  $X_2 \to Y_2$  is equivalent to simulating the transformed pair of channels  $(X_1, X_2) \to U_1$  and  $(X_1, X_2, U_1) \to U_2$ .

The mutual information of each of the original i.i.d. channels are equal to I(X;Y). However, the two transformed channels differ in terms of mutual information:  $I(X_1,X_2,U_1;U_2) > I(X;Y)$  because  $U_2$  is observed through two different channels. This necessitates that the other channel has lower mutual information:  $I(X_1,X_2;U_1) < I(X;Y)$ . Therefore, the linear transformation (6) we applied to the output had the effect of *polarizing* the target channel.

For block lengths that are larger powers of two, we can apply the transform inductively, resulting in the relationship we saw in section 2:  $U^n = Y^n G_n^{-1}$ . Similar to the two-dimensional (n=2) case, this transforms the original simulation problem  $X^n \to Y^n$  into the problem of simulating the *subchannels*  $X^n \to U_1, (X^n, U_1) \to U_2, (X^n, U_1, U_2) \to U_3, \ldots, (X^n, U^{n-1}) \to U_n$ . Arikan [2009] shows that these subchannels are polarized for large n: for each i,  $I(U_i; X^n, U^{i-1}) \approx 0$  or  $I(U_i; X^n, U^{i-1}) \approx 1$ . This allows us to simulate them using the toy algorithm described in the previous section.

Algorithms 1 and 2 describe the complete scheme.

# **Algorithm 1:** Encoder for simulating a channel using polar codes.

## **Algorithm 2:** Decoder for simulating a channel using polar codes.

```
Input :Block length n
Random bit string z^n \sim \mathrm{Unif}\,([0,1]^n)
Probability table \overline{p}^n \in [0,1]^n
Compressed offset string b
Output:Simulated channel output y^n \in \{0,1\}^n
\Delta^n \leftarrow \mathrm{Decompress}(b,\overline{p}^n)
for i=1,\ldots,n do
 | \quad \text{if } z_i > 1/2 \text{ then } v_i \leftarrow 1 \text{ else } v_i \leftarrow 0 
 | \quad u_i \leftarrow \Delta_i + v_i 
 y^n \leftarrow \mathrm{PolarEnc}(u^n) 
return y^n
```

The encoder input  $\bar{p}_i$  refers to the subchannel parameter

$$\bar{p}_i = h_B^{-1}(H(U_i|U^{i-1}, X^n)).$$
 (7)

This can be calculated offline using the techniques used to compute subchannel quality for communication described at the end of Section 2. The  $\mathtt{SoftPolarDec}(u^{i-1},x^n)$  subroutine outputs

$$\Pr(U_i = 0 | U^{i-1} = u^{i-1}, X^n = x^n), \tag{8}$$

which can be calculated with  $O(n\log n)$  complexity using a recursion given by Arikan [2009]. The PolarEnc $(u^n)$  subroutine simply multiplies by the generator matrix in:  $y^n = u^n G_n$ . This can be implemented in  $O(n\log n)$  by exploiting the recursive structure, as noted earlier. The Compress $(\Delta^n, \bar{p}^n)$  and Decompress $(b, \bar{p}^n)$  routines can be any prefix-free lossless compressor/decompressor pair that uses at most

$$c + \sum_{i=1}^{n} \left[ \mathbf{1}(\Delta_i = 1) \log \frac{1}{1/2 - \bar{p}_i} + \mathbf{1}(\Delta_i = 0) \log \frac{1}{1/2 + \bar{p}_i} \right]$$
(9)

bits to send  $\Delta^n$ , where c is some constant independent of n and  $\Delta^n$ . Arithmetic coding (Rissanen [1976]) is a widely-used scheme that achieves this guarantee with c=2.

This defines PolarSim for n that is a power of two. An arbitrary n can be handled by partitioning  $\{1,\ldots,n\}$  into subsets, each of which has a cardinality that is a power of two. One then applies PolarSim to each subset separately. Since the coding is prefix-free, the encoder outputs can simply be concatenated together, as noted in Sec. 2.1.

#### 3.3 Theoretical Guarantees

If one uses a linear complexity algorithm for Compress and Decompress, then the overall complexity of PolarSim is  $O(n\log n)$  for both encoding an decoding. Using the fact that polar codes achieve capacity for channels satisfying the symmetry condition in (4), we can show that PolarSim is rate optimal in the large-n limit, making it currently the only scheme with subexponential complexity in n with a comparable guarantee.

**Theorem 1.** Consider a joint distribution  $P_{XY}$  in which Y is binary and uniform and the reverse channel  $P_{X|Y}$  satisfies the symmetry condition in (4). Suppose Compress and Decompress achieve the guarantee in (9).

1. (Correctness:) Algorithms 1 and 2 simulate the channel  $P^{\times n}(Y|X)$  exactly: If  $Z^n$  is i.i.d. Unif [0,1], and  $\bar{p}_i = h_B^{-1}(H(U_i|U^{i-1},X^n))$ , then the conditional probability that Algorithm 2 outputs  $y^n$  given that  $x^n$  is the input to Algorithm 1 is

$$\prod_{i=1}^{n} P_{Y|X}(y_i|x_i). \tag{10}$$

2. (Optimality:) Algorithms 1 and 2 are asymptotically rate optimal:

$$\lim_{n \to \infty} \frac{1}{n} E[\ell(b)] \to I(X; Y), \tag{11}$$

where b is the output of the encoder.

The proof is provided in Appendix D.

### 3.4 Experimental Results

We run PolarSim on the reverse  $(P_{Y|X})$  version of three channels: (1) the BSC with a uniform input (2) the binary erasure channel,  $X = Z \cdot Y$ , where Y is uniform over  $\{-1,1\}$  and Z is Bernoulli( $\epsilon$ ), and (3) the binary Gaussian channel X = Y + Z, where Y is again uniform over  $\{-1,1\}$  and Z is  $\mathcal{N}(0,\sigma^2)$ . Note that the reverse of the BSC with a uniform input is the BSC itself.

Fig. 3 and Fig. 4 show the rate performance of these simulations. Even at a block length of  $2^{12}$ , the performance is already close to the mutual information lower bound across all channels and rates. Performance improves with n as expected, with both the average rate and the variance in the rate decreasing.

We also compare our scheme to the state-of-the-art scheme for channel simulation, Greedy Poisson Rejection Sampling (GPRS) [Flamich, 2024] (see Appendix E for the implementation details). Fig. 5 shows that PolarSim significantly outperforms GPRS in terms of the communication rate, even when the latter is optimized for the channel at hand. In Table 1, we can see that its computational efficiency is also significantly better, by several orders of magnitude. This is due to the exponential computational complexity of GPRS in n compared to the pseudolinear complexity of PolarSim.

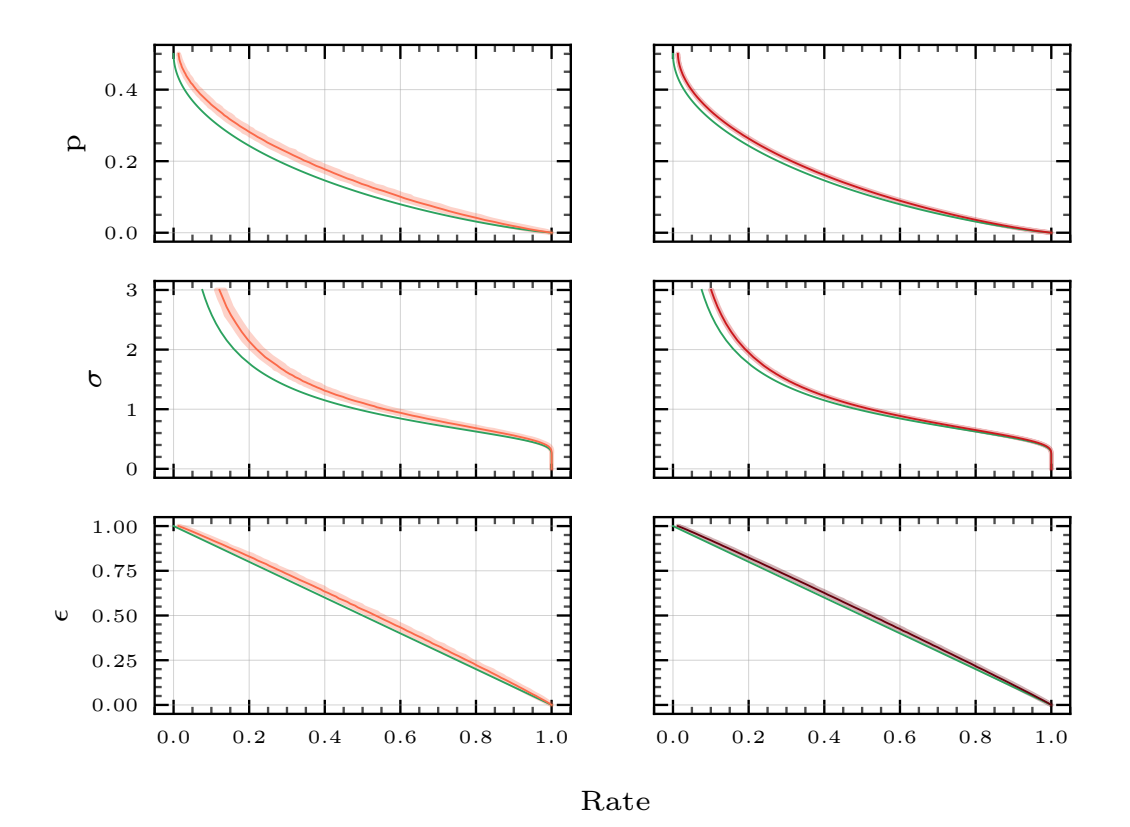


Figure 3: Rates achieved by PolarSim at different block lengths —  $\blacksquare n = 2^{12}$  (left),  $\blacksquare n = 2^{17}$  (top-right and middle-right),  $\blacksquare n = 2^{14}$  (bottom-right) for different noise levels across different channels, compared against the theoretical lower bound  $\blacksquare I(X;Y)$ . Top:  $\mathsf{BSC}_p$  for  $p \in (0,\frac{1}{2})$ , Middle: Gaussian for  $\sigma \in (0,3)$ , Bottom: Erasure for  $\epsilon \in (0,1)$ . The lines represent the median values, and the boundaries of shaded regions represent the  $5^{th}$  to  $95^{th}$  percentile rates over 200 simulation runs.

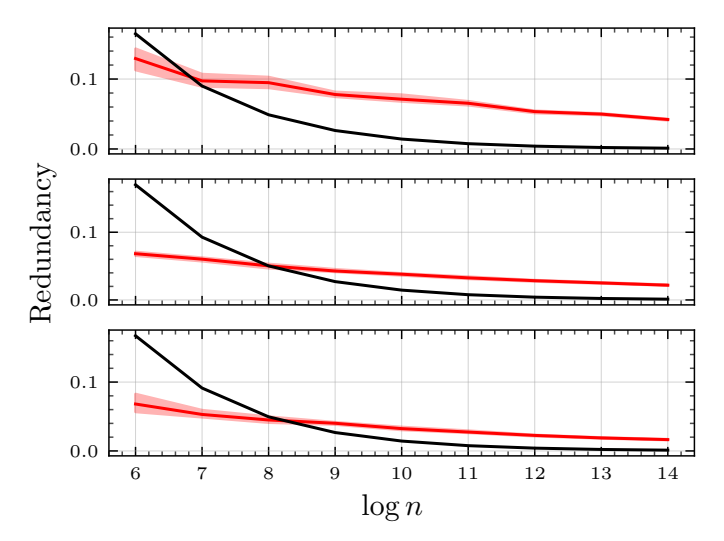


Figure 4: The redundancy of PolarSim is plotted for certain fixed channels (Top: BSC with p=0.05, Middle: Reverse binary Gaussian channel with  $\sigma=0.5$ , Bottom: Reverse binary erasure channel with  $\epsilon=0.2$ ) as the block length n is varied. The plotted curve ( $\blacksquare$ ) is the median redundancy over 200 simulations, with the boundaries of the shaded region showing the bootstrapped 95% confidence interval around the sample median. The redundancy is defined as the gap between the achieved rate and the mutual information lower bound. For comparison, the theoretical maximum redundancy of PFRL ( $\blacksquare$ ) is also plotted for the respective channels (see 3). We see that for large block lengths, PolarSim has a higher redundancy, which is consistent with known results from channel coding [Mondelli et al., 2016].

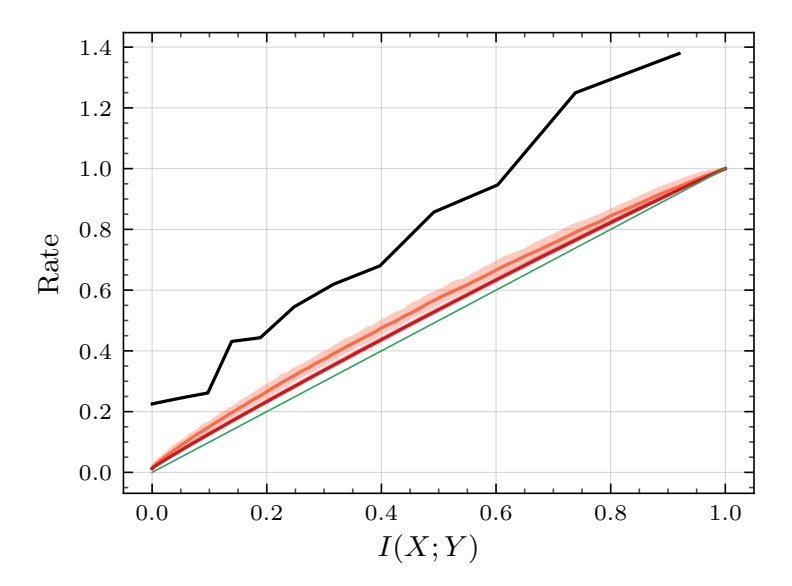


Figure 5: Comparison of schemes for BSC simulation: Average rates for PolarSim with  $\blacksquare n = 2^{12}$  and  $\blacksquare n = 2^{17}$  compared against  $\blacksquare$  GPRS with n = 8 and the theoretical lower bound  $\blacksquare I(X;Y)$  over 1000 simulation runs.

p	PolarSim			GPRS			λ
	Median	р5	p95	Median	р5	p95	
0.00	0.009	0.008	0.01	192.0	161.4	205.8	21333
0.25	0.009	0.008	0.01	246.1	180.7	415.7	27347
0.49	0.009	0.008	0.01	227.7	176.1	318.7	25305

**Table 1:** Execution time comparison between PolarSim and GPRS, for simulating BSC's with block length  $n=2^{12}$ . The reported statistics are computed over 1000 trials for each value of the crossover probability p. GPRS cannot directly simulate such large block lengths. Therefore, the GPRS runtimes are obtained by scaling up the runtime for n=8 blocks. This is justified by subadditivity (see (1)). The column  $\lambda$  computes the ratio between the medians of the two schemes. For our chosen block length, PolarSim performs over four orders of magnitude faster than GPRS.

## 4 Related Work

## 4.1 Performance Bounds

Arguably the first to consider the channel simulation problem was Wyner [1975], who studied the problem without common randomness. The problem with common randomness was first introduced in the context of quantum information theory literature by Bennett et al. [2002] and Winter [2002]. Harsha et al. [2007] proposed a greedy one-shot channel simulation algorithm that achieved a logarithmic rate redundancy with respect to the lower bound for discrete channels. Li and El Gamal [2018] showed a similar achievability result that generalizes to more general channels using their strong Poisson functional representation lemma. Sriramu and Wagner [2024] showed via a two-stage rejection sampling scheme that an even lower redundancy was achievable in the i.i.d. case. Li and Anantharam [2021] extended the Poisson representation to obtain a generalised method for deriving one-shot achievability in different settings (see also Phan et al. [2024]).

#### 4.2 Practical Schemes

The achievability proof in Li and El Gamal [2018] inspired several practical schemes that exploit properties of the Poisson process and perform well at short block lengths [Flamich et al., 2022, Flamich, 2024]. Similarly, the rejection sampler proposed by Harsha et al. [2007] has been generalized by Flamich et al. [2024] to work for arbitrary probability spaces. None of these schemes exhibit subexpoential complexity with n when applied to product channels, however. If one restricts attention

to n=1 and unimodal distributions, then improved schemes are possible [Flamich et al., 2024, Hegazy and Li, 2022], although by their nature such schemes cannot harness the amortization gain associated with increasing n.

Chou et al. [2018] addresses the problem of total variation approximate channel simulation and proposes a fixed rate scheme based on a soft covering argument that uses polar codes.

As noted in the introduction, the primary application of the channel simulation task is learned compression. Lei et al. [2024] and Li et al. [2020] consider how vector quantization methods can be directly applied to the compression task without explicitly simulating a channel. Although their methods do not simulate an i.i.d. channel, their use of ideas from error-correcting codes and vector quantization makes them the closest prior works to the present paper, along with Chou et al. [2018].

# 5 Concluding Remarks

PolarSim shows how polar codes can be used to simulate channels with favorable scalability in the dimension. By harnessing the attending amortization gain, the codes are able to realize significantly improved performance compared with existing schemes. Our focus has been on how the original form of polar codes can simulate symmetric, binary output channels. Subsequent extensions of polar codes [Şaşoğlu et al., 2009] could potentially be used to simulate arbitrary channels. This would be an interesting topic of future research.

The aim of the paper, however, is not to show that polar codes are useful for simulation *per se*. Rather, we seek to make the larger point that ideas from the field of error-correcting codes are useful for the simulation problem. We have used polar codes as an exemplar, but one could potentially apply turbo codes (Berrou et al. [1993]), low-density parity-check codes LDPCs (Gallager [1962]), algebraic codes [Blahut, 2003], trellis-coded modulation/quantization (Taubman et al. [2002]), sparse superposition codes (Joseph and Barron [2012]), or other codes (e.g., Caire et al. [1998]) instead. The PolarSim method is not expected to generalize to these other families. Polar codes are linear, however, and one can transform them into a simulator for the BSC using a different approach that relies on linearity alone. This is discussed in the supplementary materials, where we find that this alternate scheme achieves comparable performance to PolarSim. This alternate approach is directly applicable to other linear codes such as LDPCs.

In learned compression applications, the channels of interest are generally continuous. Error-correcting schemes that operate directly on continuous channels, such as trellis-coded modulation/quantization, are therefore of particular interest. To illustrate the potential of these codes, in the supplementary materials we show how trellis-coded quantization can be used to approximately simulate a Gaussian channel. The simulation is not exact, but in practical applications, exact simulation may be unnecessary.

# 6 Acknowledgement

This research was supported by the US National Science Foundation under grant CCF-2306278 and by a gift from Google. The authors wish to thank Lucas Theis and Jona Ballé for helpful discussions. They would also like to thank the anonymous reviewers for the feedback and suggestions they provided.

## References

- Gergely Flamich, Marton Havasi, and José Miguel Hernández-Lobato. Compressing images by encoding their latent representations with relative entropy coding. *Advances in Neural Information Processing Systems*, 33:16131–16141, 2020.
- Johannes Ballé, Philip A Chou, David Minnen, Saurabh Singh, Nick Johnston, Eirikur Agustsson, Sung Jin Hwang, and George Toderici. Nonlinear transform coding. *IEEE Journal of Selected Topics in Signal Processing*, 15(2):339–353, 2020.
- Marton Havasi, Robert Peharz, and José Miguel Hernández-Lobato. Minimal random code learning: Getting bits back from compressed model parameters. *International Conference on Learning Representations*, 2018.
- Abhin Shah, Wei-Ning Chen, Johannes Ballé, Peter Kairouz, and Lucas Theis. Optimal compression of locally differentially private mechanisms. *arXiv* preprint arXiv:2111.00092, 2022.
- Lucas Theis, Tim Salimans, Matthew D. Hoffman, and Fabian Mentzer. Lossy compression with Gaussian diffusion. *arXiv preprint arXiv:2206.08889*, 2022.
- Thomas M. Cover and Joy A. Thomas. *Elements of Information Theory*. John Wiley & Sons, Hoboken, 2nd edition, 2006.
- Thomas M. Liggett. Stochastic Interacting Systems: Contact, Voter and Exclusion Processes. Springer-Verlag, New York, 1999.
- Cheuk Ting Li and Abbas El Gamal. Strong functional representation lemma and applications to coding theorems. *IEEE Transactions on Information Theory*, 64(11):6967–6978, 2018.
- Prahladh Harsha, Rahul Jain, David McAllester, and Jaikumar Radhakrishnan. The communication complexity of correlation. In *Twenty-Second Annual IEEE Conference on Computational Complexity (CCC'07)*, pages 10–23. IEEE, 2007.
- Gergely Flamich, Stratis Markou, and José Miguel Hernández-Lobato. Fast relative entropy coding with A\* coding. In *International Conference on Machine Learning*, pages 6548–6577. PMLR, 2022.
- Gergely Flamich and Lucas Theis. Adaptive greedy rejection sampling. 2023 IEEE International Symposium on Information Theory (ISIT), pages 454–459, 2023.
- Gergely Flamich, Stratis Markou, and José Miguel Hernández-Lobato. Faster relative entropy coding with greedy rejection coding. *Advances in Neural Information Processing Systems*, 36, 2024.
- Ram Zamir and Meir Feder. On universal quantization by randomized uniform/lattice quantizers. *IEEE Transactions on Information Theory*, 38(2):428–436, 1992.
- Eirikur Agustsson and Lucas Theis. Universally quantized neural compression. *Advances in Neural Information Processing Systems*, 33:12367–12376, 2020.
- S.S. Pradhan, J. Chou, and K. Ramchandran. Duality between source coding and channel coding and its extension to the side information case. *IEEE Transactions on Information Theory*, 49(5): 1181–1203, 2003. doi: 10.1109/TIT.2003.810622.
- Thomas John Goblick. *Coding for a discrete information source with a distortion measure*. PhD thesis, Massachusetts Institute of Technology, 1963.
- A Viterbi and J Omura. Trellis encoding of memoryless discrete-time sources with a fidelity criterion. *IEEE Transactions on Information Theory*, 20(3):325–332, 1974.
- Rajiv Laroia, Nariman Farvardin, and Steven A Tretter. On optimal shaping of multidimensional constellations. *IEEE Transactions on Information Theory*, 40(4):1044–1056, 1994.
- Erdal Arikan. Channel polarization: A method for constructing capacity-achieving codes for symmetric binary-input memoryless channels. *IEEE Transactions on Information Theory*, 55(7): 3051–3073, 2009.

- Marco Mondelli, S Hamed Hassani, and Rüdiger L Urbanke. Unified scaling of polar codes: Error exponent, scaling exponent, moderate deviations, and error floors. *IEEE Transactions on Information Theory*, 62(12):6698–6712, 2016.
- Zeynep B Kaykac Egilmez, Luping Xiang, Robert G Maunder, and Lajos Hanzo. The development, operation and performance of the 5g polar codes. *IEEE Communications Surveys & Tutorials*, 22 (1):96–122, 2019.
- Henry Pfister. polar\_intro. https://github.com/henrypfister/polar\_intro, 2023.
- Tom Richardson and Ruediger Urbanke. Modern Coding Theory. Cambridge University Press, 2008.
- Sharang M Sriramu and Aaron B Wagner. Optimal redundancy in exact channel synthesis. *arXiv* preprint arXiv:2401.16707, 2024.
- Ido Tal and Alexander Vardy. How to construct polar codes. *IEEE Transactions on Information Theory*, 59(10):6562–6582, 2013. doi: 10.1109/TIT.2013.2272694.
- Yingxian Zhang, Aijun Liu, Kegang Pan, Chao Gong, and Sixiang Yang. A practical construction method for polar codes. *IEEE Communications Letters*, 18(11):1871–1874, 2014.
- Jorma J Rissanen. Generalized Kraft inequality and arithmetic coding. IBM Journal of research and development, 20(3):198–203, 1976.
- Gergely Flamich. Greedy Poisson rejection sampling. Advances in Neural Information Processing Systems, 36, 2024.
- A. Wyner. The common information of two dependent random variables. *IEEE Transactions on Information Theory*, 21(2):163–179, 1975. doi: 10.1109/TIT.1975.1055346.
- Charles H Bennett, Peter W Shor, John A Smolin, and Ashish V Thapliyal. Entanglement-assisted capacity of a quantum channel and the reverse Shannon theorem. *IEEE transactions on Information Theory*, 48(10):2637–2655, 2002.
- Andreas Winter. Compression of sources of probability distributions and density operators. *arXiv* preprint quant-ph/0208131, 2002.
- Cheuk Ting Li and Venkat Anantharam. A unified framework for one-shot achievability via the Poisson matching lemma. *IEEE Transactions on Information Theory*, 67(5):2624–2651, 2021.
- Buu Phan, Ashish Khisti, and Christos Louizos. Importance matching lemma for lossy compression with side information. In *International Conference on Artificial Intelligence and Statistics*, pages 1387–1395. PMLR, 2024.
- Mahmoud Hegazy and Cheuk Ting Li. Randomized quantization with exact error distribution. In *IEEE Information Theory Workshop (ITW)*, pages 350–355, 2022.
- Rémi A Chou, Matthieu R Bloch, and Jörg Kliewer. Empirical and strong coordination via soft covering with polar codes. *IEEE Transactions on Information Theory*, 64(7):5087–5100, 2018.
- Eric Lei, Hamed Hassani, and Shirin Saeedi Bidokhti. Approaching rate-distortion limits in neural compression with lattice transform coding. *arXiv preprint arXiv:2403.07320*, 2024.
- Binglin Li, Mohammad Akbari, Jie Liang, and Yang Wang. Deep learning-based image compression with trellis coded quantization. In *Data Compression Conference (DCC)*, pages 13–22, 2020.
- Eren Şaşoğlu, Emre Telatar, and Erdal Arikan. Polarization for arbitrary discrete memoryless channels. In *2009 IEEE Information Theory Workshop*, pages 144–148, 2009. doi: 10.1109/ITW. 2009.5351487.
- Claude Berrou, Alain Glavieux, and Punya Thitimajshima. Near Shannon limit error-correcting coding and decoding: Turbo-codes. 1. In *Proceedings of ICC'93-IEEE International Conference on Communications*, volume 2, pages 1064–1070. IEEE, 1993.

- Robert Gallager. Low-density parity-check codes. *IRE Transactions on information theory*, 8(1): 21–28, 1962.
- Richard E Blahut. Algebraic Codes for Data Transmission. Cambridge University Press, 2003.
- David S Taubman, Michael W Marcellin, and Majid Rabbani. Jpeg2000: Image compression fundamentals, standards and practice. *Journal of Electronic Imaging*, 11(2):286–287, 2002.
- Antony Joseph and Andrew R Barron. Least squares superposition codes of moderate dictionary size are reliable at rates up to capacity. *IEEE Transactions on Information Theory*, 58(5):2541–2557, 2012.
- Giuseppe Caire, Giorgio Taricco, and Ezio Biglieri. Bit-interleaved coded modulation. *IEEE transactions on information theory*, 44(3):927–946, 1998.
- Andrew Viterbi. Error bounds for convolutional codes and an asymptotically optimum decoding algorithm. *IEEE transactions on Information Theory*, 13(2):260–269, 1967.

# A Rate of the Toy Scheme

The rate of this scheme is governed by the cost of compressing the correction bit  $\Delta$ . We have

$$Pr(\Delta = 1) = E[Pr(\Delta = 1|X)]$$
(12)

$$= E\left[\frac{1}{2} - \min_{j \in \{0,1\}} p_{Y|X}(j|X)\right]$$
 (13)

$$= \frac{1}{2} - E \left[ \min_{j \in \{0,1\}} p_{Y|X}(j|X) \right]$$
 (14)

$$\implies H(\Delta) = h_B \left( \frac{1}{2} - E \left[ \min_{j \in \{0,1\}} p_{Y|X}(j|X) \right] \right). \tag{15}$$

Rearranging this, we can obtain

$$E\left[\min_{j\in\{0,1\}} p_{Y|X}(j|X)\right] = \frac{1}{2} - h_B^{-1}(H(\Delta)).$$
(16)

Next, consider

$$I(X;Y) = 1 - H(Y|X)$$
 (17)

$$=1-E\left[h_B\left(\min_{j\in\{0,1\}}p_{Y|X}(j|X)\right)\right] \tag{18}$$

$$\geq 1 - h_B \left( E \left[ \min_{j \in \{0,1\}} p_{Y|X}(j|X) \right] \right) \tag{19}$$

$$=1-h_B\left(\frac{1}{2}-h_B^{-1}(H(\Delta))\right). (20)$$

Rearranging this, we finally obtain the required upper bound:

$$H(\Delta) \le h_B \left(\frac{1}{2} - h_B^{-1}(1 - I(X;Y))\right).$$
 (21)

## **B** Trellis-Coded Quantization

The channel simulation scheme described in the the body of the paper is limited to binary-output channels. However, in many practical applications, we need to simulate channels with real-valued outputs. To demonstrate that the tools from coding theory are not limited to binary channels, we describe a scheme that uses *trellis coded quantization* for approximately simulating a AWGN channel for an i.i.d. Gaussian source.

The encoding algorithm for trellis coded quantization was originally developed as an efficient decoding algorithm for a family of channel coding schemes called *convolutional codes*. We will directly describe the construction used in source coding as it can be described in a self-contained manner.

A fixed-rate time-invariant trellis with k states  $\mathcal{S} = \{s_1, s_2, ..., s_k\}$  consists of a  $k \times k$  binary transition matrix G where each row and each column have exactly two nonzero entries, a set of disjoint codebooks  $\mathcal{V} = \{\mathcal{C}_1, \mathcal{C}_2, ..., \mathcal{C}_m\}$  with each containing  $2^{R-1}$  codewords from the source alphabet  $\mathcal{X}$ , and a map  $T: \{1, \ldots, k\} \times \{1, \ldots, k\} \mapsto \mathcal{V}$  which assigns a codebook to each pair of states.

A path of length n through the trellis consists of a *traversable* sequence of states  $s_t = (s_{t_0}, s_{t_1}, ..., s_{t_n})$ —i.e, all sequences such that  $G(s_{t_i}, s_{t_{i+1}}) = 1$ . For any sequence of codewords  $\hat{x}^n$ , we will use the shorthand  $\hat{x}^n \in s_t$  if  $\hat{x}^n$  can be produced by the transitions of the path—i.e., if  $\hat{x}_i \in T(s_{t_{i-1}}, s_{t_i})$  for all i.

In a data compression setting, the encoder, upon receiving a source sequence  $x^n$ , examines all traversable paths through the trellis to find a codeword sequence  $\phi(x^n)$  that is closest to  $x^n$  under the mean squared error distortion metric:

$$\phi(x^n) = \underset{\hat{x}^n \in s_0^n, \\ s_0^n \text{ is traversable}}{\arg \min} \|x^n - \hat{x}^n\|^2.$$
(22)

It then encodes this into a bit-string by specifying the sequence of state transitions used and the codeword index in the associated codebook for each transition. Our chosen structure for the transition matrix G ensures that each transition can be encoded by one bit. Each codeword can be then indexed within the corresponding codebook using R-1 bits, bringing the total communication rate to R bits per symbol.

Although the search space for finding the best codeword grows exponentially in n, it can be implemented efficiently using the *Viterbi algorithm* [Viterbi, 1967]. Here, at every stage k of our scheme, we keep track of the best paths terminating at every state s and their associated costs recursively:

$$J(s,k) = \min_{\hat{s} \in \mathcal{S}} \left( J(\hat{s}, k-1) + \min_{\hat{x} \in T(\hat{s}, s)} (x_k - \hat{x})^2 \right), \text{ and}$$

$$U(s,k) = \arg\min_{\hat{s} \in \mathcal{S}} J(s,k).$$

$$(24)$$

$$U(s,k) = \operatorname*{arg\,min}_{\hat{s} \in S} J(s,k). \tag{24}$$

The base case of the recursion is specified by the choice of the initial state  $s_{t_0}$ , which is typically set to be  $s_1$ . The initial costs are then set to be  $J(s_1,0)=0$ , and  $J(\hat{s},0)=\infty$  for all  $s_1\neq\hat{s}$ . The optimal state transition sequence and the corresponding codeword sequence  $\phi(x_1^n)$  can be recovered using  $U(\cdot,\cdot)$ .

To encode a sequence of length n, the Viterbi algorithm performs  $nm2^{R-1}$  single-letter squared distance evaluations and 2nk comparisons — thus, the computational cost grows only linearly in the block length making the algorithm highly scalable. Many practical data compression schemes use trellis codes due to this scalability, and because of their performance in terms of rate.

## **B.1** Approximate AWGN Simulation Using Trellis-Coded Quantization

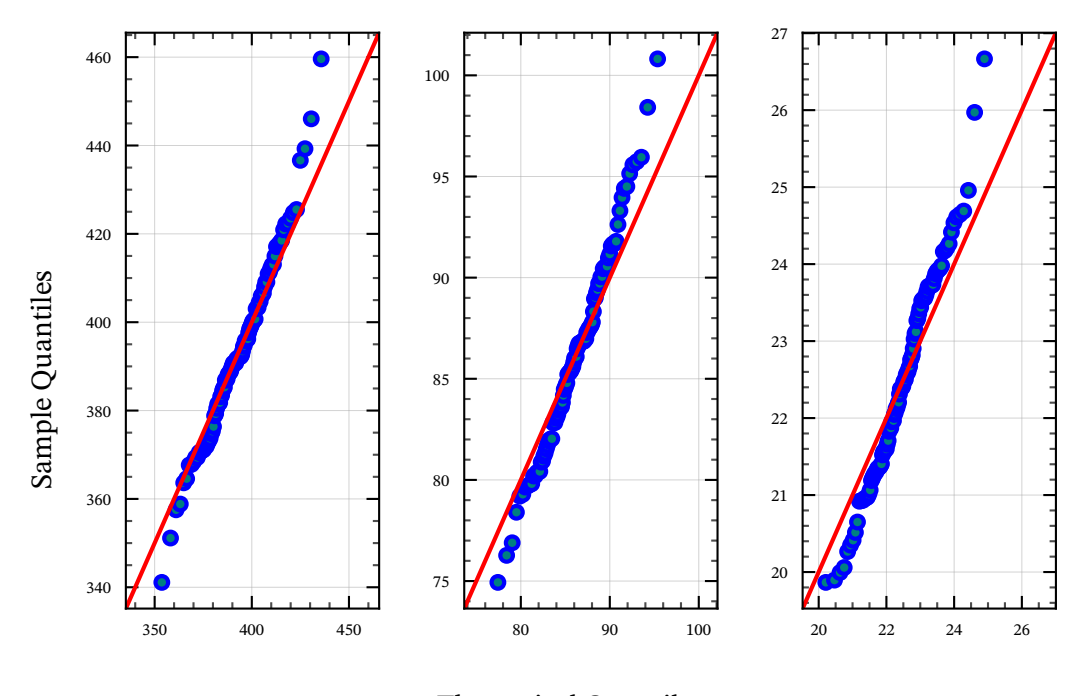
1. Let  $X^n \sim \mathcal{N}(0, \sigma^2)$  be the input at the encoder, and  $f^*(\cdot, R)$  be a rate R trellis coded quantizer that obtains an average distortion value of D. We use a 256-state trellis with each state having exactly two branches leaving it, along with a codebook of size  $2^{R+1}$  which is partitioned into 4 subsets, each of size  $2^{R-1}$ . Each branch of the trellis is then associated with one of the 4 subsets (See Figure 3.15 and Table 3.5 of Taubman et al. [2002] for a full description of the mapping used for this assignment).

The above Trellis is initialised with randomly generated codewords from a standard normal and is subsequently trained using the Lloyd-Max algorithm.

Refer to Taubman et al. [2002] for a detailed description of the Trellis construction and training.

- 2. Using the common randomness, select a uniformly random rotation matrix  $\Pi$  at both the encoder and decoder.
- 3. At the encoder, compute the randomly rotated source  $\tilde{X}^n = \Pi X^n$  and the reconstruction  $\tilde{\tilde{X}}^n = f(\tilde{X}^n, R)$ . Transmit the reconstruction to the decoder by specifying the corresponding trellis path.
- 4. Compute the scaling factor  $a=\frac{\sigma^2}{\sigma^2-D}$  and the reconstruction  $\tilde{Y}^n=a\hat{\tilde{X}}^n$
- 5. Finally, compute  $Y^n = \Pi^{-1}\tilde{Y}^n$  as the output of the channel simulation scheme. In figure 6, we generate 100 independent realizations of  $X^n$  with n = 1000 and source power  $\sigma^2 = 1$ . The scheme outlined above is then used to generate the corresponding  $Y^n$  realizations. The quantiles of the sample noise  $D = \|X^n - Y^n\|^2$  are plotted against the theoretical quantiles obtained by assuming  $p_{Y|X}$  to be AWGN with noise power  $\frac{1}{n} \sum_{i=1}^{n} \|X_i^n - Y_i^n\|^2.$

In Figure 7, we plot the rate of our approximate scheme (i.e. the rate of the trellis coded quantizer used) against the mutual information of the simulated channel. Bootstapped 95%ile confidence intervals for the mutual information are plotted to account for the error in estimating the noise power.



Theoretical Quantiles

**Figure 6:** For trellis coded quantizers with rates R=1 (**Left**), R=2 (**Middle**) and R=3 (**Right**), the quantiles for M=100 realizations of the sample noise  $D=\|Y^n-X^n\|^2$  are plotted against the theoretical quantiles obtained from an AWGN with noise power  $\frac{1}{n}$  E[D]. We use the sample mean to estimate E[D].

Using a trellis with a fixed codebook limits the output alphabet to a finite set of real numbers. To simulate a continuous channel, we introduce a random orthogonal transformation, chosen by the common randomness, that is applied to the input before encoding. The decoder subsequently applies the inverse transformation to the reconstruction. This has the effect of randomizing the output symbols while retaining their proximity to the source on average.

We present the results of this scheme in Figures 6 and 7. We see that the distribution of the realizations of the simulated channel noise are fairly close to an AWGN with matching power, and that each of the operating rates of the trellis is very close to the mutual information of the simulated channel for that rate.

# C Channel Simulation Using Arbitrary Linear Codes

Given any lattice  $\Lambda \subset \mathbb{R}^n$ , an associated quantizer  $Q_{\Lambda}$ , and a source realization  $X^n$  observed at the encoder, Zamir and Feder [1992] provide a mechanism for simulating an additive noise channel whose noise distribution is uniform over the decoding cell of the lattice,

$$Q_{\Lambda}^{-1}(0^n) = \{ z^n \in \mathbb{R} : Q_{\Lambda}(z^n) = 0^n \}, \tag{25}$$

using dithered quantization: we generate  $Z^n \sim \mathrm{Unif}(Q_\Lambda^{-1}(0^n))$  using the common randomness, and at the encoder compute  $Q_\Lambda(X^n+Z^n)$ , which is transmitted to the decoder. Then, according to Theorem 1 in Zamir and Feder [1992], computing

$$Y^n = Q_{\Lambda}(X^n + Z^n) - Z^n \tag{26}$$

recovers a sample from the target distribution. An analogous fact holds for linear codes over finite fields.

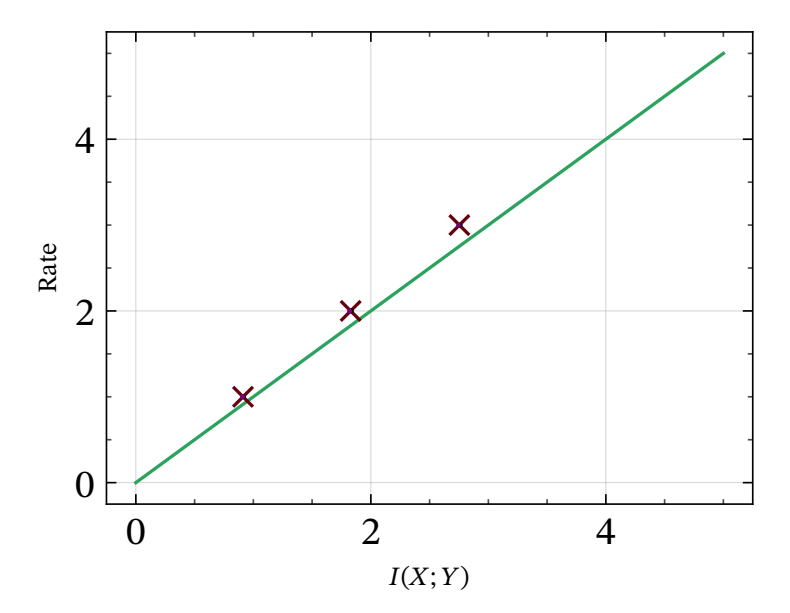


**Figure 7:** The rate of the trellis quantizer is plotted against the mutual information of the simulated channel. Bootstrapped 95% confidence intervals are plotted for the noise mean estimate.

## C.1 Alternative Scheme for the BSC Simulation Using Polar codes

For a linear code to be capacity-achieving over a channel, its decoding cell must have a certain structure. For binary codes to achieve the capacity of a BSC (such as polar codes) their decoding cells must resemble Hamming balls. Thus applying the above procedure with a polar code simulates an additive noise channel in which the noise is approximately uniformly distributed over a Hamming ball. Instead of using an additive dither to randomize the input to a deterministic quantizer, we can randomly shift the codewords to a coset of the original lattice to have the same effect. This is especially convenient for polar codes because shifting their cosets can be accomplished by randomizing the frozen bits, saving a call to the quantization routine.

Suppose we seek to simulate n uses of a BSC with crossover probability p. The number of message bits is calculated as:

$$m = n \cdot (1 - h_B(p)) \tag{27}$$

and the number of frozen bits is n-m, which are generated using the common randomness. The simulation encoder takes the input bit string  $X^n$  and the block of frozen bits. The simulation encoder runs the channel decoding algorithm with channel output  $X^n$  and the given frozen bits to obtain m message bits. These bits are passed to the simulation decoder, which runs the channel encoder to produce  $Y^n$  using the received message bits and the frozen bits. The role of the encoder and decoder as thus swapped compared to the communication task, as was the case with PolarSim (see Fig. 8). The rate of this scheme is m/n.

This scheme does not result in an exact simulation of n copies of the  $\mathsf{BSC}_p$ , however, in that  $X^n \oplus Y^n$  is uniformly distributed over the cell rather than being i.i.d. Bernoulli(p). This is both because an i.i.d. Bernoulli(p) string is not constrained to a single Hamming ball and because the cell of the polar code is not exactly a Hamming ball to begin with. Fig 9 shows a histogram of the number of bit-flips in this scheme compared with the target binomial distribution. We see that the actual distribution of bit flips (top) has a mean that is too high (because the cell is not a true Hamming ball) and a variance that is too low (because the actual noise process is not constrained to a single Hamming ball).

But we can upgrade this simulator to one that achieves exact simulation using a pre- and post-correction process. The pre-correction is to adjust the parameter of the channel simulator to be  $\hat{p} < p$ , which is chosen empirically to result in the correct (pn) number of bits being flipped on average. The post-correction scheme corrects for deviation in the variance and any remaining discrepancy in the mean and operates as follows. The encoder uses its private randomness to generate a realization of a random variable N that is binomially distributed with parameters n and p. It then runs the above

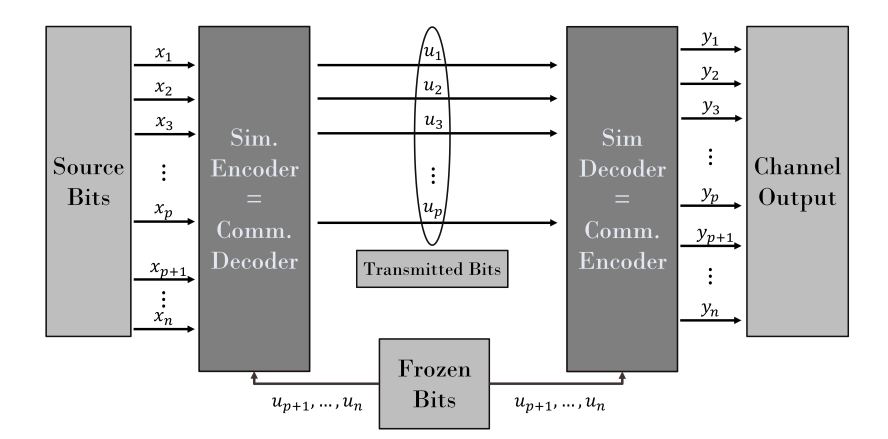


**Figure 8:** Block diagram representation of a BSC simulator based on polar codes. The role of the encoder and decoder are swapped compared with conventional communication.

process, with pre-correction, and computes the number of bits flipped by the scheme. It then sends a *correction message* to the decoder to ensure that the actual number of bits flipped is exactly N. The correction message takes two forms, depending on whether one is operating in the high-rate or low-rate regime:

- 1. If  $m < \frac{n}{2}$ : the encoder identifies the smallest L so that the first L bits of  $Y^n$  can be overwritten in such a way that the resulting  $Y^n$  string differs from  $X^n$  in exactly N positions. The encoder sends the decoder L using  $\log n$  bits and then the L bits with which the decoder should overwrite the prefix of  $Y^n$ .
- 2. If  $m \geq \frac{n}{2}$ : the encoder identifies a set of L bits that can be flipped to result in there being exactly N flipped bits overall. The encoder communicates to the decoder a binary string of length n that contains L 1's and n-L zeros. The encoder communicates L to the decoder using  $\log n$  bits. It then communicates the bit string using  $2 + \log \binom{n}{L}$  bits, which can be realized using arithmetic coding.

By construction, the post-correction scheme ensures that the noise sequence  $Z^n = X^n \oplus Y^n$  has the correct distribution. The simulator is still not exact, however, because the distribution of  $Z^n$  is not exchangeable. This can be rectified by generating a random permutation of  $\{1,\ldots,n\}$ , say  $\Pi$ , from the common randomness and having the encoder apply  $\Pi$  to  $X^n$  at the start and having the decoder apply  $\Pi^{-1}$  to  $Y^n$  at the end. Note that an exchangeable distribution over binary strings with the property that the number of ones has a binomial distribution must be i.i.d. Bernoulli.

Note that the pre-correction part of the scheme is not needed to ensure exact simulation; it only reduces the burden on the post-correction scheme. Also note that both the high-rate and low-rate schemes can be used for any value of m. We found empirically that the above division performed better than relying on either one alone. The performance of the corrected scheme is shown in (Fig. 10), which shows that the performance is similar to PolarSim. The corrected scheme can never perform better than the uncorrected scheme, but the difference between the two vanishes as n increases.

The idea of fixing the number of bit flips using the common randomness is reminiscent of the two-stage channel simulation scheme of Sriramu and Wagner [2024] and the layered randomized quantizer of Hegazy and Li [2022], which are without loss of optimality in their respective setups. Note that the above scheme can be used to simulate a BSC using any linear code if one uses the dithered approach in (26) instead of relying on frozen bits.

# D Proof of Theorem 1

**Theorem 1.** Consider a joint distribution  $P_{XY}$  in which Y is binary and uniform and the reverse channel  $P_{X|Y}$  satisfies the symmetry condition in (4). Suppose Compress and Decompress achieve the guarantee in (9).

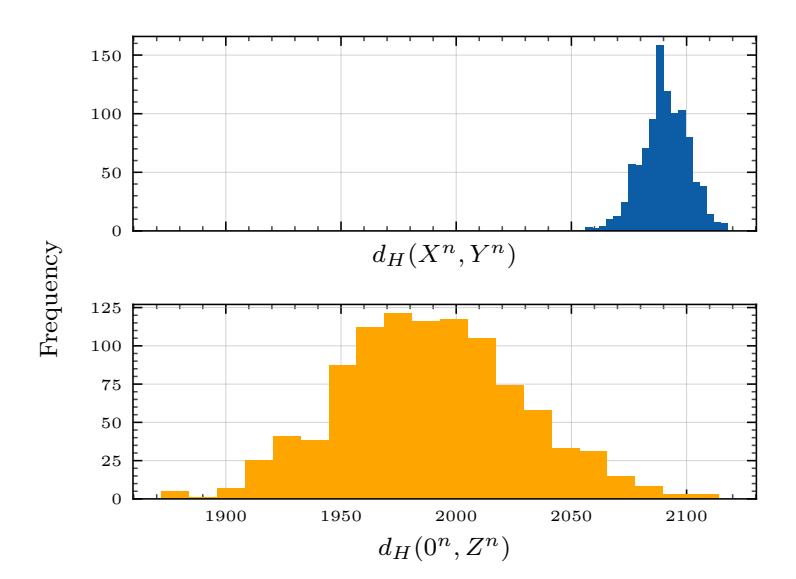


**Figure 9: Top**: The distribution of the hamming distance,  $d_H(X^n, Y^n) = \sum_{i=1}^n X_i \oplus Y_i$ , between the input binary string  $X^n$  and the output  $Y^n$  produced by the uncorrected polar simulator. **Bottom**: The target distribution, with each  $Z_i \sim \text{Bern}(p)$  i.i.d..

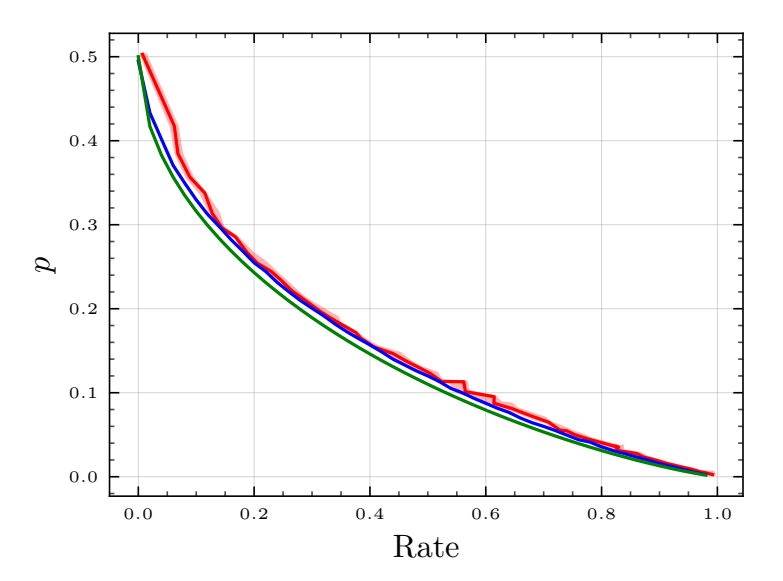


Figure 10: BSC simulation using the polar code simulator with post-correction. The median post-correction rate ( ) is plotted along with the uncorrected rate ( ) and the mutual information lower bound ( ). The boundaries of the shaded show the maximum and minimum rate for the corrected scheme over five simulation runs.

1. (Correctness:) Algorithms 1 and 2 simulate the channel  $P^{\times n}(Y|X)$  exactly: If  $Z^n$  is i.i.d.  $\mathrm{Unif}[0,1]$ , and  $\bar{p}_i=h_B^{-1}(H(U_i|U^{i-1},X^n))$ , then the conditional probability that Algorithm 2 outputs  $y^n$  given that  $x^n$  is the input to Algorithm 1 is

$$\prod_{i=1}^{n} P_{Y|X}(y_i|x_i). \tag{28}$$

2. (Optimality:) Algorithms 1 and 2 are asymptotically rate optimal:

$$\lim_{n \to \infty} \frac{1}{n} E[\ell(b)] \to I(X; Y), \tag{29}$$

where b is the output of the encoder

*Proof.* Suppose n is a power of two, and consider the following joint distribution between  $(U^n, X^n, Y^n)$ :

$$\Pr(U^n = u^n, Y^n = y^n, X^n = x^n) = \prod_{i=1}^n P_X(x_i) \prod_{i=1}^n P_{Y|X}(y_i|x_i) 1(u^n = y^n G^{-1})$$
 (30)

$$= \frac{1}{2^n} 1(y^n = u^n G) \prod_{i=1}^n P_{X|Y}(x_i|y_i).$$
 (31)

Given the input  $X^n$ , the  $U^n$  string generated by the encoder has distribution  $P_{U|X}^{\times n}$  by construction, since SoftPolarDec $(x^n,u^{i-1},P_{X|Y})$  computes  $\Pr(U_i=0|X^n=x^n,U^{i-1}=u^{i-1})$  under the distribution in (30)-(31). Due to the lossless nature of the compression,  $\Delta^n$  is recovered exactly at the decoder. Since  $V^n$  is common to the two terminals,  $U^n$  is thus recovered exactly by the decoder. Then setting  $Y^n=U^n\cdot G$  results in  $(X^n,Y^n)$  having the joint distribution  $P_{XY}^{\times n}$  as desired. This establishes the correctness of the algorithm for n that is a power of two. Correctness of the algorithm for any n immediately follows.

Turning to optimality, again suppose n is a power of two. For the sequence  $\Delta^n$  we have

$$\Pr(\Delta_i = 1) = \frac{1}{2} - \sum_{u^{i-1}, x^n} P_{U^{i-1}, X^n}(u^{i-1}, x^n) \min\left(\Pr(U_i = 1 | U^{i-1} = u^{i-1}, X^n = x^n), (32)\right)$$

$$\Pr(U_i = 0 | U^{i-1} = u^{i-1}, X^n = x^n))$$

(33)

$$= \frac{1}{2} - \sum_{u^{i-1}, x^n} P_{U^{i-1}, X^n}(u^{i-1}, x^n) h_B^{-1}(H(U_i|U^{i-1} = u^{i-1}, X^n = x^n))$$
(34)

$$\leq \frac{1}{2} - h_B^{-1}(H(U_i|U^{i-1}, X^n)) \tag{35}$$

$$=\frac{1}{2}-\bar{p}_i,\tag{36}$$

where the inequality follows by the convexity of  $h_B^{-1}(\cdot)$ . Thus the average rate may be bounded as

$$\frac{1}{n} \operatorname{E}[\ell(b)] \le \frac{1}{n} \sum_{i=1}^{n} \left[ \Pr(\Delta_i = 1) \log \frac{1}{1/2 - \bar{p}_i} + \Pr(\Delta_i = 0) \log \frac{1}{1/2 + \bar{p}_i} \right] + \frac{c}{n}$$
(37)

$$\leq \frac{1}{n} \sum_{i=1}^{n} h_B \left( \frac{1}{2} - \bar{p}_i \right) + \frac{c}{n}. \tag{38}$$

We bound this quantity using the polarization property. Fix  $\delta > 0$ . By Arikan [2009], for all sufficiently large n there is a set  $\mathcal{N}_n$  of "noisy" indices such that

$$\frac{|\mathcal{N}_n|}{n} \ge 1 - I(X;Y) - \delta \tag{39}$$

$$h_B(1/2 - \bar{p}_i) \le \delta \quad \text{for all } i \in \mathcal{N}_n.$$
 (40)

The rate is thus upper bounded by

$$\frac{E[\ell(b)]}{n} \le \frac{n - |\mathcal{N}_n|}{n} + \frac{1}{n} \sum_{i \in \mathcal{N}_n} h_B(1/2 - \bar{p}_i) + \frac{c}{n}$$
(41)

$$\leq \frac{n - |\mathcal{N}_n|}{n} + \frac{\delta \cdot |\mathcal{N}_n|}{n} + \frac{c}{n}$$

$$\leq I(X;Y) + 2\delta + \frac{c}{n}.$$

$$(42)$$

$$\leq I(X;Y) + 2\delta + \frac{c}{n}. (43)$$

If we let  $\bar{R}_n = \mathrm{E}[\ell(b)]/n$  denote the minimum rate of PolarSim at block length n (minimized over all partitions if it is not a power of two), then  $n\bar{R}_n$  is itself subadditive. As n increases through powers of two, from (43) we have

$$\bar{R}_n \to I(X;Y).$$
 (44)

and thus

$$\inf_{n} \bar{R}_n = I(X;Y). \tag{45}$$

The result then follows by subadditivity (cf. 1).

#### $\mathbf{E}$ **GPRS Implementation Details**

We implement Algorithm 3 from Flamich [2024]. The proposal distribution P is chosen to be i.i.d. Bernoulli(1/2) with n=8. Given the input  $X^n=x^n$ , the target distribution  $Q(y^n)$  is chosen to be  $\prod_{i=1}^n \mathsf{BSC}_p(y_i|x_i)$ , where p ranges over (0,1/2). The stretch function  $\sigma$  was derived using the definitions provided in [Flamich 2023]:

$$\begin{split} w_P(h) &= F\left(\frac{\log h - n(\log(1-p)+1)}{\log p - \log(1-p)}, n, \frac{1}{2}\right), \\ w_Q(h) &= F\left(\frac{\log h - n(\log(1-p)+1)}{\log p - \log(1-p)}, n, p\right), \text{ and} \\ \sigma(h) &= \int\limits_0^h \frac{1}{w_Q(\eta) - \eta w_P(\eta)} d\eta, \end{split}$$

where  $F(\cdot, n, p)$  is the CDF of a Binomial(n, p) random variable. This stretch function was evaluated numerically for each input.

The algorithm outputs a positive integer n, which is entropy coded using the Zeta distribution in [Flamich 2023, (151)]. The number of bits is divided by n = 8 to obtain the rate. For each p on a grid in  $(0,\frac{1}{2})$ , we run the simulation 200 times and plot the average rate obtained against the channel mutual information 1 - H(p).

We now make use of the fact that the selection rule employed by the algorithm needs to be evaluated for each point in the output sample space only once — if the first occurrence of an output sequence in the randomly generated codebook is rejected, all its subsequent occurrences are also rejected. This simplification helps speed up the execution significantly and also reduces the rate as repetitions need not be indexed.

# **NeurIPS Paper Checklist**

#### 1. Claims

Question: Do the main claims made in the abstract and introduction accurately reflect the paper's contributions and scope?

Answer: [Yes]

Justification: The paper shows how ideas from error-correcting codes can be applied to the channel simulation problem, resulting in significantly improved performance in both rate and computational complexity. Both the strengths and limitations of approach are noted in the abstract and the introduction.

#### Guidelines:

- The answer NA means that the abstract and introduction do not include the claims made in the paper.
- The abstract and/or introduction should clearly state the claims made, including the
  contributions made in the paper and important assumptions and limitations. A No or
  NA answer to this question will not be perceived well by the reviewers.
- The claims made should match theoretical and experimental results, and reflect how much the results can be expected to generalize to other settings.
- It is fine to include aspirational goals as motivation as long as it is clear that these goals
  are not attained by the paper.

#### 2. Limitations

Question: Does the paper discuss the limitations of the work performed by the authors?

Answer: [Yes]

Justification: Our main scheme can perform nearly rate-optimal channel simulation highly efficiently, but it is restricted to symmetric binary output channels. We make this clear even in the abstract. Our other scheme, using Trellis Coded Quantization, does not guarantee exact simulations. We make it clear that it is an approximate simulator in our description.

#### Guidelines:

- The answer NA means that the paper has no limitation while the answer No means that the paper has limitations, but those are not discussed in the paper.
- The authors are encouraged to create a separate "Limitations" section in their paper.
- The paper should point out any strong assumptions and how robust the results are to violations of these assumptions (e.g., independence assumptions, noiseless settings, model well-specification, asymptotic approximations only holding locally). The authors should reflect on how these assumptions might be violated in practice and what the implications would be.
- The authors should reflect on the scope of the claims made, e.g., if the approach was only tested on a few datasets or with a few runs. In general, empirical results often depend on implicit assumptions, which should be articulated.
- The authors should reflect on the factors that influence the performance of the approach. For example, a facial recognition algorithm may perform poorly when image resolution is low or images are taken in low lighting. Or a speech-to-text system might not be used reliably to provide closed captions for online lectures because it fails to handle technical jargon.
- The authors should discuss the computational efficiency of the proposed algorithms and how they scale with dataset size.
- If applicable, the authors should discuss possible limitations of their approach to address problems of privacy and fairness.
- While the authors might fear that complete honesty about limitations might be used by reviewers as grounds for rejection, a worse outcome might be that reviewers discover limitations that aren't acknowledged in the paper. The authors should use their best judgment and recognize that individual actions in favor of transparency play an important role in developing norms that preserve the integrity of the community. Reviewers will be specifically instructed to not penalize honesty concerning limitations.

#### 3. Theory Assumptions and Proofs

Question: For each theoretical result, does the paper provide the full set of assumptions and a complete (and correct) proof?

Answer: [Yes]

Justification: Theorem 1 is stated with all necessary assumptions and has a complete proof in the appendix.

# Guidelines:

- The answer NA means that the paper does not include theoretical results.
- All the theorems, formulas, and proofs in the paper should be numbered and crossreferenced.
- All assumptions should be clearly stated or referenced in the statement of any theorems.
- The proofs can either appear in the main paper or the supplemental material, but if they appear in the supplemental material, the authors are encouraged to provide a short proof sketch to provide intuition.
- Inversely, any informal proof provided in the core of the paper should be complemented by formal proofs provided in appendix or supplemental material.
- Theorems and Lemmas that the proof relies upon should be properly referenced.

#### 4. Experimental Result Reproducibility

Question: Does the paper fully disclose all the information needed to reproduce the main experimental results of the paper to the extent that it affects the main claims and/or conclusions of the paper (regardless of whether the code and data are provided or not)?

Answer: [Yes]

Justification: We describe our algorithm and experimental setup in detail, and also include code as part of our supplementary material.

#### Guidelines:

- The answer NA means that the paper does not include experiments.
- If the paper includes experiments, a No answer to this question will not be perceived well by the reviewers: Making the paper reproducible is important, regardless of whether the code and data are provided or not.
- If the contribution is a dataset and/or model, the authors should describe the steps taken to make their results reproducible or verifiable.
- Depending on the contribution, reproducibility can be accomplished in various ways. For example, if the contribution is a novel architecture, describing the architecture fully might suffice, or if the contribution is a specific model and empirical evaluation, it may be necessary to either make it possible for others to replicate the model with the same dataset, or provide access to the model. In general, releasing code and data is often one good way to accomplish this, but reproducibility can also be provided via detailed instructions for how to replicate the results, access to a hosted model (e.g., in the case of a large language model), releasing of a model checkpoint, or other means that are appropriate to the research performed.
- While NeurIPS does not require releasing code, the conference does require all submissions to provide some reasonable avenue for reproducibility, which may depend on the nature of the contribution. For example
- (a) If the contribution is primarily a new algorithm, the paper should make it clear how to reproduce that algorithm.
- (b) If the contribution is primarily a new model architecture, the paper should describe the architecture clearly and fully.
- (c) If the contribution is a new model (e.g., a large language model), then there should either be a way to access this model for reproducing the results or a way to reproduce the model (e.g., with an open-source dataset or instructions for how to construct the dataset).
- (d) We recognize that reproducibility may be tricky in some cases, in which case authors are welcome to describe the particular way they provide for reproducibility.

In the case of closed-source models, it may be that access to the model is limited in some way (e.g., to registered users), but it should be possible for other researchers to have some path to reproducing or verifying the results.

# 5. Open access to data and code

Question: Does the paper provide open access to the data and code, with sufficient instructions to faithfully reproduce the main experimental results, as described in supplemental material?

Answer: [Yes]

Justification: We include code as part of our supplementary material with instructions on how to run it.

#### Guidelines:

- The answer NA means that paper does not include experiments requiring code.
- Please see the NeurIPS code and data submission guidelines (https://nips.cc/public/guides/CodeSubmissionPolicy) for more details.
- While we encourage the release of code and data, we understand that this might not be possible, so "No" is an acceptable answer. Papers cannot be rejected simply for not including code, unless this is central to the contribution (e.g., for a new open-source benchmark).
- The instructions should contain the exact command and environment needed to run to reproduce the results. See the NeurIPS code and data submission guidelines (https://nips.cc/public/guides/CodeSubmissionPolicy) for more details.
- The authors should provide instructions on data access and preparation, including how to access the raw data, preprocessed data, intermediate data, and generated data, etc.
- The authors should provide scripts to reproduce all experimental results for the new proposed method and baselines. If only a subset of experiments are reproducible, they should state which ones are omitted from the script and why.
- At submission time, to preserve anonymity, the authors should release anonymized versions (if applicable).
- Providing as much information as possible in supplemental material (appended to the paper) is recommended, but including URLs to data and code is permitted.

# 6. Experimental Setting/Details

Question: Does the paper specify all the training and test details (e.g., data splits, hyper-parameters, how they were chosen, type of optimizer, etc.) necessary to understand the results?

Answer: [Yes]

Justification: Our algorithm description and the descriptions of our results are detailed enough to be reproducible. One of the virtues of the PolarSim is that there are no hyperparameters to choose.

#### Guidelines:

- The answer NA means that the paper does not include experiments.
- The experimental setting should be presented in the core of the paper to a level of detail that is necessary to appreciate the results and make sense of them.
- The full details can be provided either with the code, in appendix, or as supplemental
  material.

#### 7. Experiment Statistical Significance

Question: Does the paper report error bars suitably and correctly defined or other appropriate information about the statistical significance of the experiments?

Answer: [Yes]

Justification: The main plots that show the performance of PolarSim and the post-correction scheme include error bars. Error bars were not included for the competitor schemes, PFRL and GPRS, due to their computational complexity. As noted in the paper, GPRS does not even consistently run to completion in a reasonable time for some parameter values.

#### Guidelines:

- The answer NA means that the paper does not include experiments.
- The authors should answer "Yes" if the results are accompanied by error bars, confidence intervals, or statistical significance tests, at least for the experiments that support the main claims of the paper.
- The factors of variability that the error bars are capturing should be clearly stated (for example, train/test split, initialization, random drawing of some parameter, or overall run with given experimental conditions).
- The method for calculating the error bars should be explained (closed form formula, call to a library function, bootstrap, etc.)
- The assumptions made should be given (e.g., Normally distributed errors).
- It should be clear whether the error bar is the standard deviation or the standard error
  of the mean.
- It is OK to report 1-sigma error bars, but one should state it. The authors should preferably report a 2-sigma error bar than state that they have a 96% CI, if the hypothesis of Normality of errors is not verified.
- For asymmetric distributions, the authors should be careful not to show in tables or figures symmetric error bars that would yield results that are out of range (e.g. negative error rates).
- If error bars are reported in tables or plots, The authors should explain in the text how they were calculated and reference the corresponding figures or tables in the text.

# 8. Experiments Compute Resources

Question: For each experiment, does the paper provide sufficient information on the computer resources (type of compute workers, memory, time of execution) needed to reproduce the experiments?

Answer: [Yes]

Justification: It is noted in the paper that all experiments were run on a consumer-grade CPU. It is also noted that PolarSim for n=1024 takes less than 0.1 seconds per run. The context makes clear that the runtime for other experiments and channels are similar.

#### Guidelines:

- The answer NA means that the paper does not include experiments.
- The paper should indicate the type of compute workers CPU or GPU, internal cluster, or cloud provider, including relevant memory and storage.
- The paper should provide the amount of compute required for each of the individual experimental runs as well as estimate the total compute.
- The paper should disclose whether the full research project required more compute than the experiments reported in the paper (e.g., preliminary or failed experiments that didn't make it into the paper).

#### 9. Code Of Ethics

Question: Does the research conducted in the paper conform, in every respect, with the NeurIPS Code of Ethics https://neurips.cc/public/EthicsGuidelines?

Answer: [Yes]

Justification: All authors received prevailing wages or course credit for their contributions to the paper. The paper is methodological and does not involve any datasets or human subjects.

## Guidelines:

- The answer NA means that the authors have not reviewed the NeurIPS Code of Ethics.
- If the authors answer No, they should explain the special circumstances that require a deviation from the Code of Ethics.
- The authors should make sure to preserve anonymity (e.g., if there is a special consideration due to laws or regulations in their jurisdiction).

# 10. Broader Impacts

Question: Does the paper discuss both potential positive societal impacts and negative societal impacts of the work performed?

Answer: [NA]

Justification: This paper presents foundational research that is not expected to directly lead to societal impacts. It could lead to improved compression schemes for various types of data, which would certainly be a positive societal impact. This impact is implicit in the introduction.

#### Guidelines:

- The answer NA means that there is no societal impact of the work performed.
- If the authors answer NA or No, they should explain why their work has no societal impact or why the paper does not address societal impact.
- Examples of negative societal impacts include potential malicious or unintended uses (e.g., disinformation, generating fake profiles, surveillance), fairness considerations (e.g., deployment of technologies that could make decisions that unfairly impact specific groups), privacy considerations, and security considerations.
- The conference expects that many papers will be foundational research and not tied to particular applications, let alone deployments. However, if there is a direct path to any negative applications, the authors should point it out. For example, it is legitimate to point out that an improvement in the quality of generative models could be used to generate deepfakes for disinformation. On the other hand, it is not needed to point out that a generic algorithm for optimizing neural networks could enable people to train models that generate Deepfakes faster.
- The authors should consider possible harms that could arise when the technology is being used as intended and functioning correctly, harms that could arise when the technology is being used as intended but gives incorrect results, and harms following from (intentional or unintentional) misuse of the technology.
- If there are negative societal impacts, the authors could also discuss possible mitigation strategies (e.g., gated release of models, providing defenses in addition to attacks, mechanisms for monitoring misuse, mechanisms to monitor how a system learns from feedback over time, improving the efficiency and accessibility of ML).

#### 11. Safeguards

Question: Does the paper describe safeguards that have been put in place for responsible release of data or models that have a high risk for misuse (e.g., pretrained language models, image generators, or scraped datasets)?

Answer: [NA]

Justification: The paper does not involve datasets of any kind. All experiments were run on synthetically generated data.

#### Guidelines:

- The answer NA means that the paper poses no such risks.
- Released models that have a high risk for misuse or dual-use should be released with
  necessary safeguards to allow for controlled use of the model, for example by requiring
  that users adhere to usage guidelines or restrictions to access the model or implementing
  safety filters.
- Datasets that have been scraped from the Internet could pose safety risks. The authors should describe how they avoided releasing unsafe images.
- We recognize that providing effective safeguards is challenging, and many papers do
  not require this, but we encourage authors to take this into account and make a best
  faith effort.

# 12. Licenses for existing assets

Question: Are the creators or original owners of assets (e.g., code, data, models), used in the paper, properly credited and are the license and terms of use explicitly mentioned and properly respected?

Answer: [Yes]

Justification: Other than our own code, we used Dr. Henry Pfister's polar code implementation (https://github.com/henrypfister/polar\_intro) on GitHub which is available under the 'GNU Affero General Public License v3.0' license that places no restrictions on its usage. In our code, we have clearly mentioned which parts are derived from his code.

#### Guidelines:

- The answer NA means that the paper does not use existing assets.
- The authors should cite the original paper that produced the code package or dataset.
- The authors should state which version of the asset is used and, if possible, include a URL.
- The name of the license (e.g., CC-BY 4.0) should be included for each asset.
- For scraped data from a particular source (e.g., website), the copyright and terms of service of that source should be provided.
- If assets are released, the license, copyright information, and terms of use in the package should be provided. For popular datasets, paperswithcode.com/datasets has curated licenses for some datasets. Their licensing guide can help determine the license of a dataset.
- For existing datasets that are re-packaged, both the original license and the license of the derived asset (if it has changed) should be provided.
- If this information is not available online, the authors are encouraged to reach out to the asset's creators.

#### 13. New Assets

Question: Are new assets introduced in the paper well documented and is the documentation provided alongside the assets?

Answer: [Yes]

Justification: We provide the code we used to run our experiments along with instructions on how to run it.

#### Guidelines:

- The answer NA means that the paper does not release new assets.
- Researchers should communicate the details of the dataset/code/model as part of their submissions via structured templates. This includes details about training, license, limitations, etc.
- The paper should discuss whether and how consent was obtained from people whose asset is used.
- At submission time, remember to anonymize your assets (if applicable). You can either create an anonymized URL or include an anonymized zip file.

# 14. Crowdsourcing and Research with Human Subjects

Question: For crowdsourcing experiments and research with human subjects, does the paper include the full text of instructions given to participants and screenshots, if applicable, as well as details about compensation (if any)?

Answer: [NA]

Justification: Because the research presented in this paper involved neither crowdsourcing nor human study participants, this criteria is not applicable.

# Guidelines:

- The answer NA means that the paper does not involve crowdsourcing nor research with human subjects.
- Including this information in the supplemental material is fine, but if the main contribution of the paper involves human subjects, then as much detail as possible should be included in the main paper.
- According to the NeurIPS Code of Ethics, workers involved in data collection, curation, or other labor should be paid at least the minimum wage in the country of the data collector.

# 15. Institutional Review Board (IRB) Approvals or Equivalent for Research with Human Subjects

Question: Does the paper describe potential risks incurred by study participants, whether such risks were disclosed to the subjects, and whether Institutional Review Board (IRB) approvals (or an equivalent approval/review based on the requirements of your country or institution) were obtained?

Answer: [NA]

Justification: Because the research presented in this paper involved neither crowdsourcing nor human study participants, this criteria is not applicable.

#### Guidelines:

- The answer NA means that the paper does not involve crowdsourcing nor research with human subjects.
- Depending on the country in which research is conducted, IRB approval (or equivalent)
  may be required for any human subjects research. If you obtained IRB approval, you
  should clearly state this in the paper.
- We recognize that the procedures for this may vary significantly between institutions and locations, and we expect authors to adhere to the NeurIPS Code of Ethics and the guidelines for their institution.
- For initial submissions, do not include any information that would break anonymity (if applicable), such as the institution conducting the review.